



Seismic Performance Evaluation of Large-Size Suspended Ceiling Using an Array of Shake Tables

S.-C. Jun⁽¹⁾, C.-H. Lee^{(2)*}, C.-J. Bae⁽³⁾, S.-Y. Kim⁽⁴⁾, K.-J. Lee⁽⁵⁾

⁽¹⁾ Graduate student, Dept. of Architecture and Architectural Engineering, Seoul National University, Seoul 08826, Republic of Korea, corrora90@snu.ac.kr

⁽²⁾ Professor, Dept. of Architecture and Architectural Engineering, Seoul National University, Seoul 08826, Republic of Korea, ceholee@snu.ac.kr (corresponding author)

⁽³⁾ Graduate student, Dept. of Architecture and Architectural Engineering, Seoul National University, Seoul 08826, Republic of Korea, changjun0125@snu.ac.kr

⁽⁴⁾ Assistant Professor, School of Architecture, Changwon National University, Changwon 51140, Republic of Korea, sungyong.kim7@gmail.com

⁽⁵⁾ System Development & Quality Team Manager, USG Boral Korea Co., Ltd., Seoul 06164, Republic of Korea, kyung-joo.lee@usgboral.com

Abstract

Recent earthquakes around the world have clearly demonstrated the critical role of nonstructural elements in maintaining the functionality of buildings and even keeping the life safety of residents. Suspended ceiling systems are among the most frequently reported earthquake-vulnerable nonstructural elements. Despite their importance, suspended ceiling systems are still designed empirically rather than by well-established engineering procedure because of their complex construction details and behavior. In this study, in order to evaluate the ceiling performance more realistically, dynamic tests of large-size suspended ceiling systems comparable to actual constructed size were conducted using an array of two shake tables. A test frame having overall dimension of 13m (length) x 5m (width) x 3m (height) was designed and constructed using three modular segments: two 5m x 5m square frames installed on the top of two shake tables and a 3m x 5m link segment which connects the two square frames rigidly. The test frame was designed sufficiently stiff in order to avoid unintended amplification of input motion at the test frame roof. Additionally, a total of five smaller specimens were tested under critical input motions. The specimens were prepared as a free-floating system by allowing free movements at the four edges according to conventional practice in Korea. Based on test results, some of the key engineering parameters including the acceleration amplification factor and the natural frequency were identified and overall seismic performances were evaluated. Compared to the extensive failure observed in the lay-in panel ceiling specimens, relatively minor damages around the pounded edge were observed for the continuous panel ceiling specimens due to the continuous restraining effects of screw-attached panels on the grid members. The test results showed that the median amplification factor for the suspended ceiling systems was about 2.02 and 1.50 respectively for each vertical and horizontal directions, lower than the ASCE 7 value for flexible components. The dynamic behavior of the tested suspended ceilings hung by long hanger bolts was very different from that of ideal pendulum. Because of the unidirectional rotation-restraining nature of the hanger bolt connection, different behavior was observed in each orthogonal direction. The natural frequencies of the tested suspended ceilings were well predicted when the deformed shape of hanger bolt was modeled as a single curvature bending in rotation-free direction and a double curvature bending in rotation-restrained direction.

Keywords: nonstructural elements, suspended ceiling, large-scale dynamic test, seismic performance evaluation



1. Introduction

Seismic damages reported during past major earthquakes have repeatedly demonstrated that significant property and functional losses, even serious injuries and casualties can result from the poor performance of non-structural elements even though they are not part of the main structural system.

Failure of suspended ceiling is among one of the most earthquake-vulnerable non-structural elements. During the recent 2016 Gyeongju and 2018 Pohang earthquakes in South Korea, the failure of suspended ceiling systems caused the functionality loss of many buildings and threatened life safety (Fig.1). However, suspended ceiling systems are still being designed empirically rather than based on a well-established engineering procedure because of their complex details and behaviors.

The seismic performance of suspended ceiling systems has been evaluated in several previous studies. Most of these research efforts have focused on producing the seismic fragility data of the typical ceiling systems through shake table testing. Although these test results gave many useful implications regarding seismic performance of suspended ceilings, their physical behavior and dynamic characteristics such as natural frequency and damping ratio are not well known yet.

In this study, in order to better understand seismic behavior of suspended ceiling systems and obtain useful design information, uniaxial dynamic tests of large-size suspended ceiling systems comparable to actual constructed size were conducted using an array of two shake tables. The dynamic tests of smaller size ceiling systems were also conducted in order to evaluate multi-directional input effects. A total of five ceiling specimens having diverse configurations were fabricated according to typical practices considered in Korea. From the dynamic test results, their physical behavior and some of the key dynamic properties were analyzed and the damage states observed at each stage of the test were presented.

2. Suspended Ceiling System

A suspended ceiling system is usually composed of hanger members, ceiling panels, wall moldings and ceiling grids. There exist many types of suspended ceiling systems. They can be classified based on the types of grid members used to construct ceiling grids and hanger members (hanger wires or bolts) to hang the entire ceiling grid to the structural floor above. In this study, four types of ceiling systems were considered. The key characteristics of each ceiling system are summarized in this section.

One of the suspended ceiling systems popular worldwide is composed of hanger wires and ceiling grids system fabricated with main T-beams and cross T-beams. Ceiling panels are usually placed within the ceiling grid without any positive attachments to grid members (lay-in ceiling). This system is also called a direct hung suspended ceiling system since the hanger wires are directly looped through holes in main T-beams and connected to the floor above [see Fig.2 (a)].



(a) Failure of continuous panel ceiling system

(b) Failure of lay-in panel ceiling system

Fig. 1 – Damages of suspended ceilings observed in Gyeongju (Mw = 5.4) and Pohang (Mw = 5.4) earthquakes in Korea



In Korea, also in Japan, along with the direct hung suspended ceiling system, several different types of suspended ceiling systems are commonly used. The major differences are the hanger members and details to connect ceiling grids to the floor above. Fig.2 (b) shows the details of a suspended ceiling system. In this system, the main T-beams in the ceiling grids are attached to additional C-section members, often called a carrying channel, with C/T clips. Instead of hanger wires, hanger bolts are used to connect the grid system to the floor slab. Since the entire ceiling grid is hung through the carrying channel, it is also classified as an indirect hung suspended ceiling system.

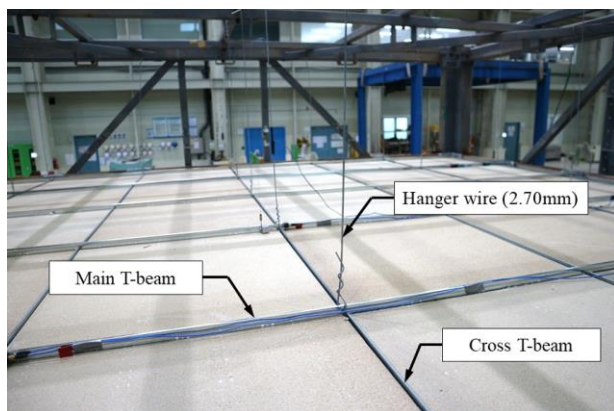
A ceiling grid system consisting of main T-beams, cross T-beams and additional cross H-beams is also widely used in many commercial buildings. In this grid system, cross T-beams and cross H-beams are installed between the main T-beams as shown in Fig.2 (c). Unlike the cross T-beams, which is connected to the main T-beams, cross H-beams do not have any positive connection with the main T-beams.

In the case of continuous panel ceiling systems, a grid system consisting of M-section members (M-beam) is widely used. As shown in Fig.2 (d), the grid is formed without any cross members and ceiling panels are screw-attached to the M-beams.

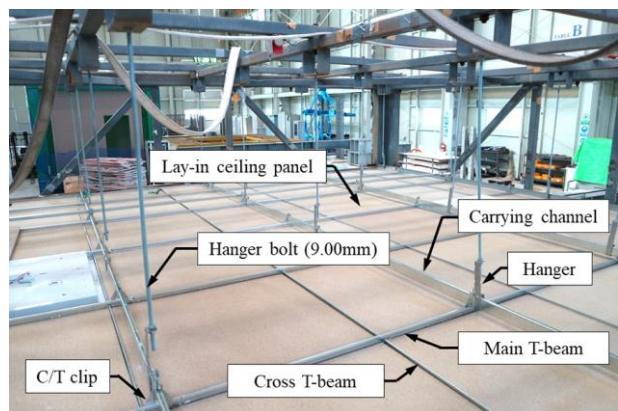
3. Experimental program

3.1 Shake table test frames for large size suspended ceiling systems

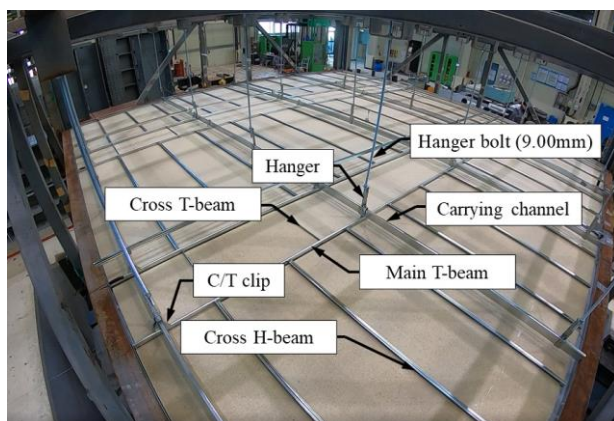
In this study, in order to conduct dynamic tests of large-size suspended ceiling systems comparable to actual



(a) Direct hung suspended ceiling system (T-beam)
(Lay-in panel)



(b) Indirect hung suspended ceiling system (T-beam)
(Lay-in panel)

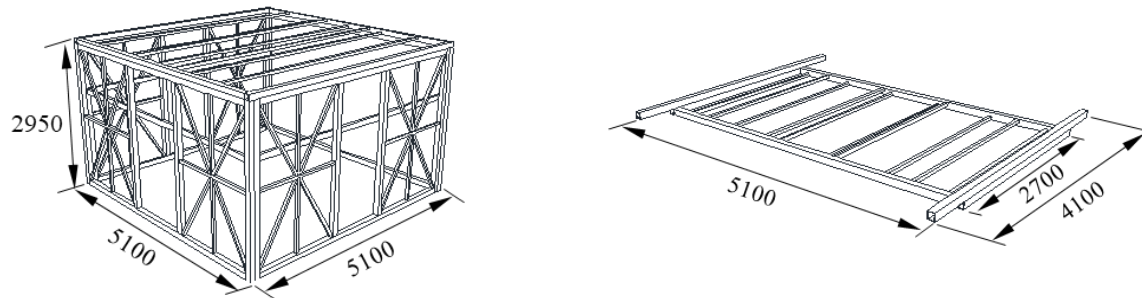


(c) Indirect hung suspended ceiling system (T&H-beam)
(Lay-in panel)



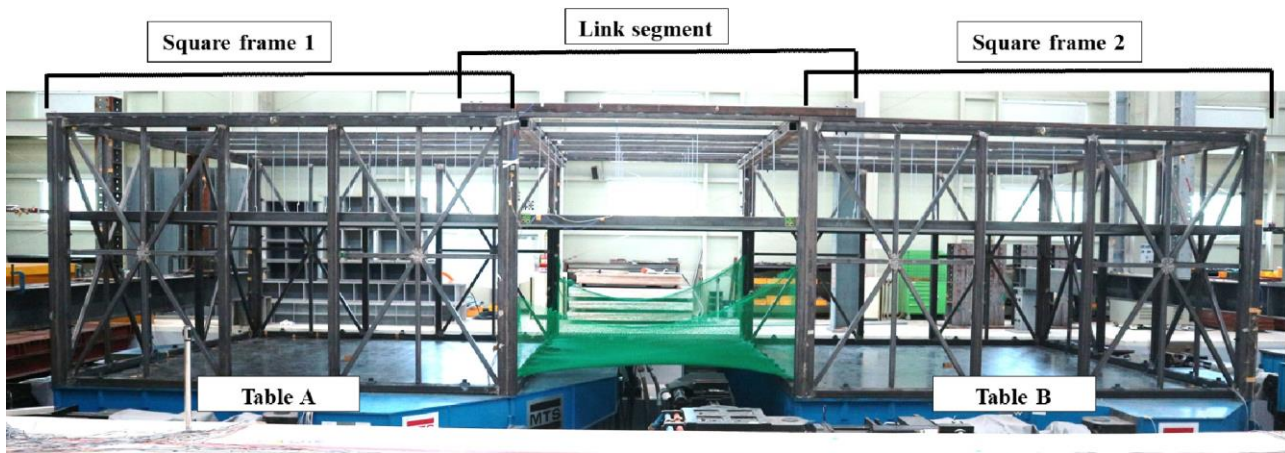
(d) Indirect hung suspended ceiling system (M-beam)
(Continuous panel)

Fig. 2 – Suspended ceiling systems used in South Korea



(a) Square frame 1 and 2 mounted on shake table

(b) Link segment connecting two square frames



(c) Overview of large-size test frame

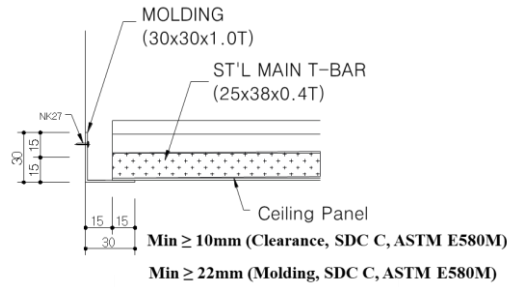
Fig. 3 – Large-size test frame for shake table testing of suspended ceiling systems and modular segments

constructed size, the large-size test frame was designed and fabricated as shown in Fig.3. The overall dimension of large-size test frame was 13.1m (length) x 5.1m (width) x 3m (height) constructed using three modular segments: two 5.1m x 5.1m square frames installed on the array of shake tables and a 4.1m x 5.1m link segment which connects the two square frames rigidly. The test frame was designed to have sufficient stiffness. The test frame was designed to have a natural frequency of 24Hz for each bare square frame and 17Hz for the combined test frame including the mass of ceiling specimens. The natural frequency measured from the white noise test was 16.8Hz for the whole test frame which was deemed sufficiently stiff to avoid unintended amplification of table input motion at the test frame roof.

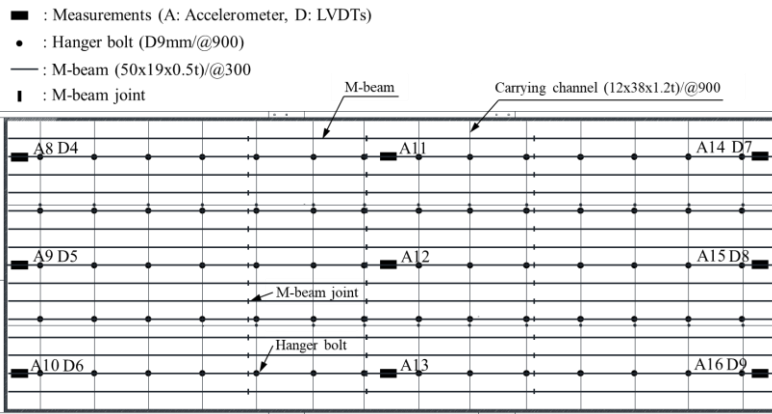
Small-size tests were also conducted to supplement the large-size test and evaluate the multi-directional input effects 3.9m (length) x 3.9m (width) x 3.0m (height) test frame mounted on single shake tables. The natural frequencies of small-size test frames were measured to be 23 Hz in each horizontal direction and 9.4 Hz in vertical direction.

3.2 Test specimens

A total of 5 suspended ceiling specimens, one large-size ceiling (12.8m x 4.85m in plan) and four small-size ceilings (3.79m x 3.79m in plan), were fabricated with including four types of suspended ceiling systems discussed in the previous section. As shown in Fig.4 (a), all the boundaries of test specimens were treated to have a 15mm clearance between the grid members and wall in order to satisfy a minimum requirement (10mm) for Seismic Design Category C (non-seismic details) of ASTM E580M (ASTM E580M, 2017). Key specimen information is summarized in Table 1.



(a) Ceiling boundary details for all tested specimens



(b) Configuration of IMC-L specimen

Fig. 4 – Ceiling boundary details and configuration of IMC-L specimen

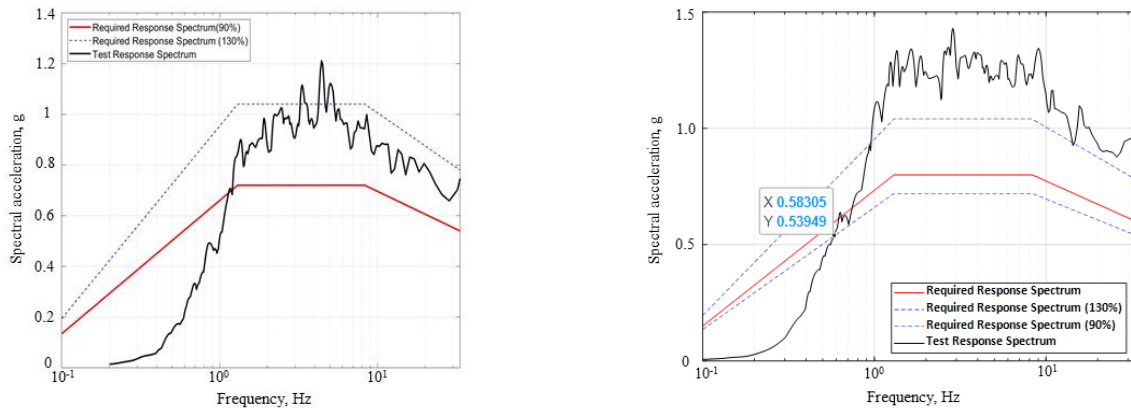
In this experimental program, direct and indirect T-beam ceiling systems (DTC & ITC) were tested to investigate the differences in their dynamic properties and seismic performance. For continuous panel ceiling (IMC-L), uniaxial dynamic tests were performed using a large-size test frame described in the preceding section [see Fig.4 (b)]. In order to evaluate the 3-D effects and the interaction with a secondary element, small-size test specimens were also prepared by installing the air conditioner within a ceiling specimen (IMC).

3.4 Loading protocol

Shake table tests were conducted according to the loading protocol suggested by ICC-ES-AC 156 (ICC,

Table 1 – Ceiling types and key properties of test specimens

Specimen	Ceiling type	Ceiling size (m)	Input motion	Boundary Type	Plenum height (m)	Panel Type
DTC	Direct hung suspended T-beam Ceiling	3.79x3.79	x, y, z	4-end free (15mm clearance)	0.75	Lay-in
ITC	Indirect hung suspended T-beam Ceiling	3.79x3.79	x, y, z	4-end free (15mm clearance)	0.75	Lay-in
ITHC	Indirect hung suspended T&H-beam Ceiling	3.79x3.79	x, y, z	4-end free (15mm clearance)	0.75	Lay-in
IMC-L	Indirect hung suspended M-beam Ceiling (Large-size)	12.8x4.85	x	4-end free (15mm clearance)	1.00	Continuous
IMC	Indirect hung suspended M-beam Ceiling	3.79x3.79	x, y, z	4-end free (15mm clearance)	0.75	Continuous



(a) TRS for indirect suspended ceiling specimens

(b) TRS for direct suspended ceiling specimen

Fig. 5- Test Response Spectrum (TRS) measured at the top of test frames

2010), which is widely used to evaluate the seismic performance of non-structural elements. Artificial ground motions were generated to match the required response spectrum (RRS) developed from the two parameters, story height ratio ($z/h = 1.0$) and design spectral response acceleration at short periods ($S_{DS} = 0.5g$) which corresponds to the highest seismic demand according to Korean Building Code. Fig.5 shows the RRS and the test response spectrum (TRS) obtained from the acceleration data measured at the top of test frames. For test specimens to be qualified using the ICC-ES-AC 156 protocol, the TRS is required to envelop the RRS down to 75 percent of the lowest resonance frequency at test specimens. As will be discussed later, for DTC specimen, a very low frequency was expected due to its pendulum behavior. Therefore, the TRS was matched to the RRS as low as possible allowed by the shake table [see Fig.5 (b)].

4. Test results

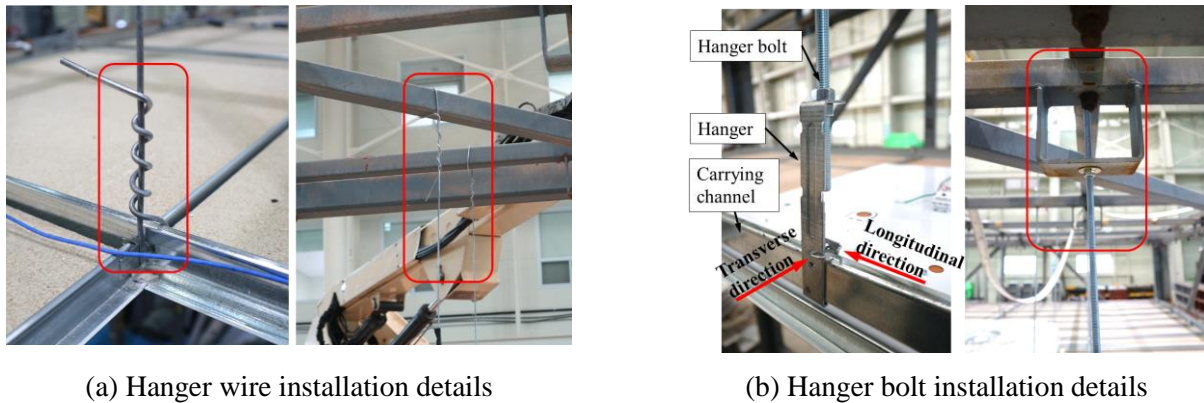
4.1 Fundamental period of suspended ceiling

In this section, the natural frequency of the tested suspended ceilings was analyzed and the behavioral characteristics of each specimen were discussed which can be used to predict the natural frequency of ceiling systems.

The resonance frequency search was conducted through the white noise and sine sweep tests. For the resonance frequency search tests, additional specimens were fabricated which have a wider clearance (410mm) between the ceiling boundary and the wall in uniaxial (ITC-R1) and biaxial (ITC-R2) directions. Such clearance was introduced to eliminate the unwanted acceleration amplification of ceiling specimens caused by pounding upon the wall molding.

For direct T-beam ceiling specimen (DTC), the natural frequency was measured to be 0.56Hz. It is close to the natural frequency calculated using the pendulum theory as reported in previous studies (Yao, 2000 and Pourali et al., 2017). In the case of indirect ceiling specimens (ITC, ITC-1, ITC-2, IMC-L) relatively higher natural frequency was obtained. In particular, it was observed that the ceiling specimen showed a different natural frequency in its orthogonal directions. For example, in the case of ITC specimen, the natural frequency measured was 1.50Hz and 4.82Hz in each orthogonal direction.

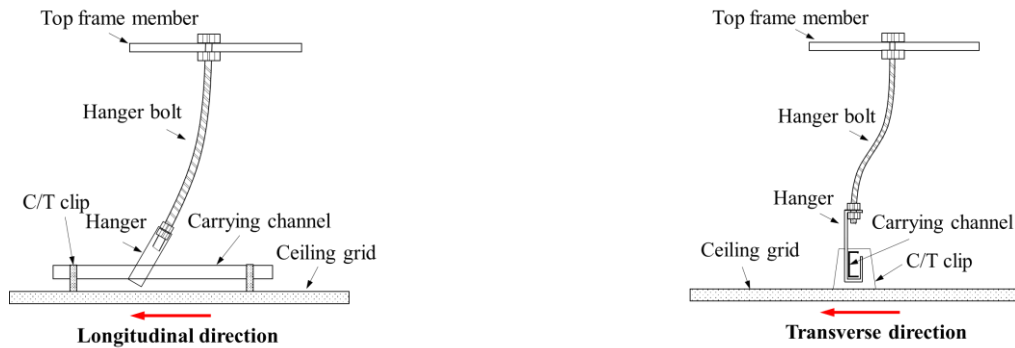
The difference in the natural frequency of these two systems was caused by the difference in installing and fastening the hanger members. As shown in Fig.6, the hanger wire was looped through the holes in the grid members in the one end and the other end was looped around the roof members of the test frame. Therefore, the hanger wire was free to rotate at both ends, thus allowing direct suspended ceiling system to respond like a pendulum. In the case of the indirect suspended ceiling, the rotational movement of the hanger bolt was



(a) Hanger wire installation details

(b) Hanger bolt installation details

Fig.6 – Comparison of installation details between hanger wire and hanger bolt



(a) Behavior of hanger bolt in rotation free direction

(b) Behavior of hanger bolt in rotation restrained direction

Fig.7 – Behavior of hanger bolt in its rotation free and restrained directions

restrained at the roof level in both directions (see Fig.6). However, at the grid level, the rotational movement of hanger bolt was restrained only in one direction (see Fig.7). When the ceiling system was excited to the rotation free direction, the hanger bolt showed a single curvature bending deformation. But excited to the rotation-restrained direction, a double curvature bending deformation was observed in the hanger bolt due to the restraining effect of hanger bolt at both ends. Therefore, the indirect suspended ceiling showed higher natural frequency in its rotation-restrained direction.

In order to mechanically model the observed behavior of the indirect suspended ceiling, the natural frequency was determined by calculating the stiffness of hanger bolt based on single and double curvature bending deformations. The stiffness of hanger bolt can be obtained as follows,

$$k = \frac{3EI}{L^3} \quad (\text{for single curvature bending})$$

$$= \frac{12EI}{L^3} \quad (\text{for double curvature bending})$$
(1)

Thus, the natural frequency of the indirect suspended ceiling can be determined as follows,

$$f_n = \frac{1}{2\pi} \sqrt{\frac{k}{m}}$$
(2)

where k = lateral stiffness of a single hanger bolt, and m = mass of ceiling system carried by a single hanger bolt.



Table 2 – Comparison of natural frequencies based on measured and calculated results

Specimen	$f_{n,measured}$ (Longitudinal)	$f_{n,measured}$ (Transverse)	$f_{n,calculated}$ (Longitudinal)	$f_{n,calculated}$ (Transverse)	Remark
DTC	0.56Hz	0.55Hz	0.56Hz	0.56Hz	Pendulum system
ITC	1.5Hz	4.75Hz	1.54Hz	4.44Hz	Single (Long.) & Double (Trans.) curvature bending
ITC-R1	1.5Hz	-	1.54Hz	-	Single curvature bending
ITC-R2	1.5Hz	-	1.54Hz	-	Single curvature bending
IMC-L	2.57Hz	2.57Hz	2.67Hz	-	Double curvature bending

Note: Longitudinal = perpendicular to direction of carrying channel; Transverse = parallel to direction of carrying channel

Table 2. compares the measured natural frequencies and the predicted ones calculated using Eq (1) and Eq (2). It is observed that the natural frequencies of the tested suspended ceilings are well predicted by the single and double curvature bending models proposed in this study.

4.2 Acceleration Amplification Factor

The acceleration amplification factor of ceiling specimens was also measured. Table 3 summarizes the median amplification factor obtained from the acceleration data measured at grid members. Low-pass filter with a cut-off frequency of 10Hz was applied to the measured acceleration data in obtaining the amplification factors.

Compared with the component amplification factor given by ASCE 7-16, for flexible components ($a_p = 2.5$), most of the specimens showed lower amplification factors in both horizontal and vertical directions. Compiling all the data, the median amplification factor was obtained as 2.02 and 1.55 respectively for horizontal and vertical directions.

Table 3 – Median amplification factors obtained from shake table test

Specimen	Amplification factor, a_p		
	x-dir.	y-dir.	z-dir.
DTC	1.85	2.27	2.50
ITC	1.96	2.01	1.38
ITHC	2.40	2.44	1.55
IMC-L	2.45	-	-
IMC	1.58	1.63	1.24

4.2 Damage observation

Direct hung suspended T-beam ceiling (DTC) specimen (lay-in panel ceiling)

Table 4 summarizes the accumulated damages of the DTC specimen observed during tests. In DTC specimen, due to the low in-plane stiffness of ceiling grids and the weak cross T-beam connections, substantial damage was observed. The perimeter ceiling panel damage caused by the failure of perimeter cross T-beams triggered torsional irregularity on the grid system which in turn caused the ceiling specimen to undergo torsional behavior. Due to the torsional effect, the inner grid members and panels started to fail rapidly. At the end of the test about 30% of ceiling panels were failed (see Fig. 8)

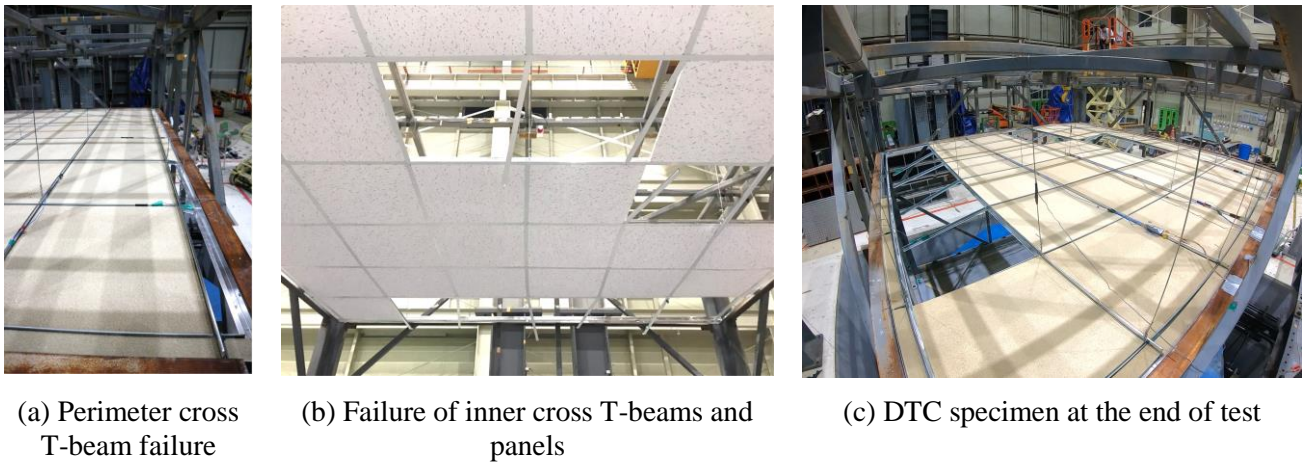


Fig. 8 – Failure pattern of direct hung T-beam ceiling (DTC) specimen

Indirect T-beam suspended ceiling system (ITC) specimen (lay-in panel ceiling)

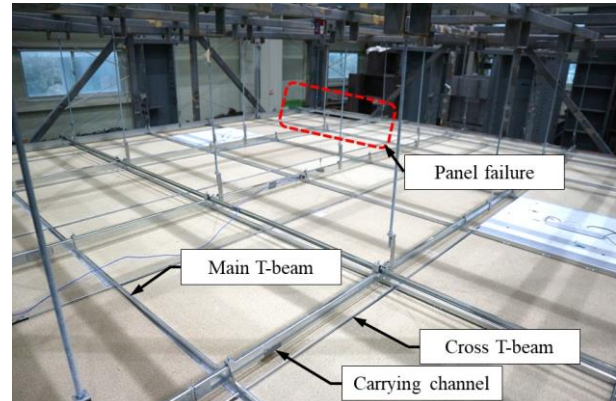
In the case of ITC specimen, much less damage was observed compared to DTC specimen. No damage was observed until $PGA = 0.71g$. Similar to DTC specimen, the failure of perimeter cross T-beams caused the perimeter ceiling panel failure (Fig.9). However, no damage was observed in the inner grid members even after the specimen experienced higher intensity ground motions than DTC specimen. It is thought that the main reason for the less damage observed in ITC specimen is due to the presence of carrying channels across the main T-beams [Fig.9 (b)]. The carrying channels which connects main T-beams along the whole length of the ceiling, served as a restraint for cross T-beams which were shown to be the weakest link in DTC specimen.

Table 4 – Accumulated damages observed from direct hung suspended T-beam ceiling (DTC) specimen

Specimen	Input PGA (g)			Damage observations
	x-dir.	y-dir.	z-dir.	
DTC	0.31	0.24	0.09	-
	0.48	0.35	0.14	perimeter cross T-beam connection failure (2 ea.) (14%)
	0.65	0.46	0.18	perimeter cross T-beam connection failure (4 ea.) (29%)
	0.69	0.53	0.22	perimeter cross T-beam connection failure (5 ea.) (36%)
	0.86	0.64	0.25	perimeter cross T-beam connection failure (5 ea.) (36%) perimeter ceiling panel failure (3 ea.) (0.7%)
	1.05	0.77	0.28	perimeter cross T-beam connection failure (9 ea.) (64%) cross T-bar connection failure (3 ea.) (7%) perimeter & center ceiling panel failure (5 ea.) (3 ea.) (10%)
	1.24	0.89	0.31	perimeter cross T-beam connection failure (14 ea.) (100%) cross T-bar connection failure (6 ea.) (14%) perimeter & center ceiling panel failure (8 ea.) (6 ea.) (18%)
1.43	1.03	0.38	perimeter cross T-beam connection failure (14 ea.) (100%) cross T-bar connection failure (12 ea.) (29%) perimeter & center ceiling panel failure (10 ea.) (10 ea.) (29%)	



(a) Failure of perimeter cross T-beams and Panels



(b) ITC specimen at the end of test

Fig. 9 – Failure pattern of indirect hung T-beam ceiling (ITC) specimen

Indirect T&H-beam suspended ceiling (ITHC) specimen (lay-in panel ceiling)

The earliest failure in this testing program was observed in the ITHC specimen. As shown in Fig.9 (a), at a low intensity loading ($PGA = 0.57g$), most of the panels were unseated from the main T-beams. As mentioned previously, cross H-beams do not have any positive connection with main T-beams. Once the panels started to fail, rapid progressive failure of entire panels at the perimeter was observed as shown in Fig.9 (b). At the end of the test, about 40% of ceiling panels were failed.

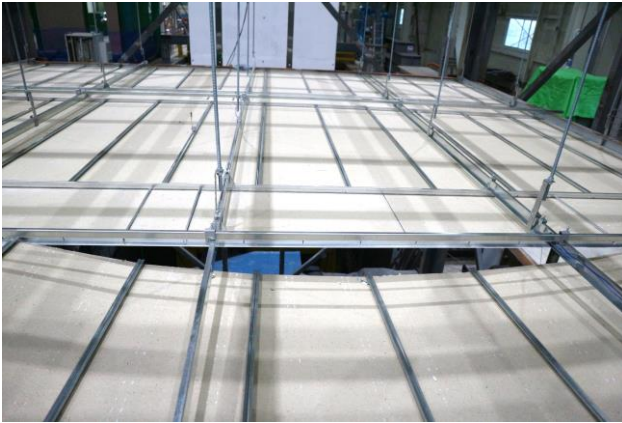
Indirect M-beam suspended ceiling (IMC and IMC-L) specimen (continuous panel ceiling)

In contrast to the lay-in panel ceiling systems, continuous panel ceiling specimens (IMC and IMC-L specimens) experienced much less damage because of the continuous restraining effects provided by the screw-attached panels on the grid members. In the case of uniaxial large-size ceiling specimen (IMC-L) only minor damage was observed until the end of test ($PGA = 1.86g$). Damage includes partial failure of perimeter ceiling panels, molding damage and panel failure (1 ea.) as shown in Fig.11 (a).

In tri-axial test specimen with air conditioner installed (IMC), although not severe, more damage was observed compared to IMC-L specimen. At the end of test ($PGA = 1.61g$), failure of perimeter ceiling panels (2 ea.) and ceiling screw was observed as shown in Fig.11 (b). Especially, at the ceiling perimeter on the same grid line with the location of air conditioner, concentrated partial failure of ceiling panels was occurred probably because of accumulated inertia effect there.

Table 5 – Accumulated damages observed from indirect hung suspended T-beam ceiling (ITC) specimen

Specimen	Input PGA (g)			Damage observations
	x-dir.	y-dir.	z-dir.	
ITC	0.84	0.79	0.40	perimeter cross T-beam connection failure (1 ea.) (7%)
	0.96	0.86	0.48	perimeter cross T-beam connection failure (1 ea.) (7%)
	1.11	1.02	0.54	perimeter cross T-beam connection failure (2 ea.) (14%)
	1.23	1.16	0.61	perimeter cross T-beam connection failure (2 ea.) (14%)
	1.48	1.42	0.71	perimeter cross T-beam connection failure (2 ea.) (14%)
	1.54	1.49	0.80	perimeter cross T-beam connection failure (2 ea.) (14%) perimeter ceiling panel failure (2 ea.)



(a) Failure of perimeter cross T-beams and Panels



(b) ITC specimen at the end of test

Fig. 10 – Failure of indirect hung T&H-beam ceiling (ITHC) specimen during dynamic test



(a) Observed failure in IMC-L specimen (partial panel, molding, panel failure)



(b) Observed failure in IMC specimen (panel, screw, perimeter panel failure)

Fig. 11 – Failure pattern of continuous panel ceiling specimen

Table 6 – Accumulated damages observed from indirect hung suspended T&H-beam ceiling (ITHC) specimen

Specimen	Input PGA (g)			Damage observations
	x-dir.	y-dir.	z-dir.	
ITHC	0.57	0.55	0.29	ceiling panel unseating
	0.72	0.74	0.33	ceiling panel unseating
	0.85	0.87	0.49	ceiling panel failure (3 ea.) (7%)
	0.97	0.97	0.38	ceiling panel failure (9 ea.) (20%)
	1.09	1.14	0.50	ceiling panel failure (18 ea.) (41%)
	1.27	1.32	0.54	ceiling panel failure (18 ea.) (41%)



5. Summary and conclusions

In this study, uniaxial dynamic tests of large-size suspended ceiling systems comparable to actual constructed size were conducted using an array of two shake tables. The shake-table tests of smaller size ceiling systems were also conducted in order to evaluate multi-directional input effects. Based on the dynamic tests of various suspended ceiling systems, their seismic performance, physical behavior and some of the key dynamic properties were analyzed. The results of this study can be summarized as follows.

(1) The analysis of the natural frequency of test specimens, clearly indicated that the behavior of suspended ceilings depends on the connection details of hanger members. Direct suspended ceiling specimen, hung by hanger wires, showed a pendulum behavior since both ends of the hanger wire were free to rotate. Indirect suspended ceiling specimens, hung by hanger bolts, showed relatively higher natural frequency due to the rotation-restrained details used between the hanger bolt and frame top. Because of the unidirectional rotation-restrained detail used between the hanger bolt and the grid system, single and double curvature bending deformations were observed for each orthogonal direction. The calculated natural frequency of test specimens using single and double curvature bending models showed good agreement with the measured natural frequency. These behavioral characteristics found in direct and indirect hung suspended ceiling systems are essential for developing standard engineering design procedure for such ceiling systems.

(2) The measured amplification factors generally showed lower values, than the factor given by ASCE 7-16, for both horizontal and vertical directions. The median amplification factors were measured to be 2.02 and 1.55 respectively for horizontal and vertical directions.

(3) Direct-hung T-beam ceiling specimen showed substantial damage mainly caused by the early damage of cross T-beams and its low in-plane stiffness. In indirect-hung T-beam ceiling specimens, much less damage was observed even after the specimens experienced stronger input motions. This was possibly due to the presence of the carrying channels in indirect-hung specimens. The carrying channels restrained the cross T-beams which became easily unstable in the direct-hung ceiling system. In the large-size continuous panel ceiling specimen, only minor damage was observed because of the continuous restraining effects provided by screw-attached panels on the grid members. However, in the tri-axial input specimen with air conditioner installed, although not severe, more damage was observed especially at the ceiling perimeter on the same grid line with the location of air conditioner.

6. Acknowledgement

This research was supported by a grant (20AUDP-C146352-03) from Architecture & Urban Development Research Program funded by Ministry of Land, Infrastructure and Transport of Korean government.

7. References

- [1] ASTM-E580/ASTM-E580M-17 (2017): *Standard Practice for Installation of Ceiling Suspension Systems for Acoustical Tile and Lay-in Panels in Area Subjected to Earthquake Ground Motions*, ASTM International, West Conshohocken, Pennsylvania.
- [2] ICC Evaluation Service (2010): *Acceptance Criteria for Seismic Certification by Shake-Table Testing of Nonstructural Components*. AC156. Whittier, CA: ICC Evaluation Service.
- [3] Yao, GC (2000): Seismic Performance of Direct Hung Suspended Ceiling Systems. *Journal of Architectural Engineering*, **6** (1), 6-11.
- [4] Pourali A, Dhakal, RP, MacRae G, Tasligedik S (2017): Fully-floating suspended ceiling system: experimental evaluation of structural feasibility and challenges. *Earthquake Spectra*, **33** (4), 1627-1654.